Autonomous Power Line Inspection with Drones via Perception-Aware MPC

Jiaxu Xing*, Giovanni Cioffi*, Javier Hidalgo-Carrió, and Davide Scaramuzza

***Abstract*— Drones have the potential to revolutionize power line inspection by increasing productivity, reducing inspection time, improving data quality, and eliminating the risks for human operators. Current state-of-the-art systems for power line inspection using drones have two shortcomings: (i) control is decoupled from perception and needs accurate information about the location of the power lines and masts; (ii) obstacle avoidance is decoupled from the power line tracking, which results in poor tracking in the vicinity of the power masts, and, consequently, in decreased data quality for visual inspection. In this work, we propose a model predictive controller (MPC) that overcomes these limitations by tightly coupling perception and action. Our controller generates commands that maximize the visibility of the power lines while, at the same time, safely avoiding the power masts. For power line detection, we propose a lightweight learning-based detector that is trained only on synthetic data and is able to transfer zero-shot to real-world power line images.**

Video: `https://youtu.be/JA6h-Nv29pU`

I. Introduction

Drones exhibit the potential to bring about a revolutionary transformation in the industrial inspection market [1], [2]. Particularly, quadrotors are a fast-to-deploy and cost-effective solution for power line inspection. The EU and US power systems consist of more than 10 million km of power lines and distribution transformers, which connect more than 400 million customers [3], [4]. The power line infrastructure needs to be inspected regularly to avoid power outages and natural disasters (California's second-largest wildfire was sparked when power lines came in contact with a tree [5]).

State-of-the-art autonomous systems for power line inspection have two shortcomings: (i) Control and motion planning are separated from perception, and they also require precise information regarding the location of power lines and masts. This information is only available in limited cases. (ii) Collision avoidance and power line tracking are decoupled, which could lead to losing track of the power lines after successfully avoiding an obstacle. For further details, we refer the reader to a survey on autonomous, vision-based robotic inspection of power lines [6].

We propose a vision-based, tightly-coupled perception and action solution for autonomous power line inspection that does not require prior information about the power line infrastructure, such as the location of the power lines and masts. Our method plans and tracks a trajectory that maximizes the visibility of the power line in the onboard-camera view and, at the same time, can safely avoid obstacles such as the power masts. We achieve this by developing a perception-aware Model Predictive Controller (MPC) [7] that includes two perception objectives: one for line tracking and one for collision avoidance. Adding multiple, and possibly conflicting, perception objectives in the MPC is a challenging task. In particular, the optimization could become infeasible and computationally intractable on resource-constrained platforms such as quadrotors. We overcome this problem by letting the MPC optimize over the weights of the two perception objectives *online*.

To detect the power lines, we propose a novel perception module that extends the deep-learning–based object detector in [8] to the case of power line detection. The perception module is trained only on synthetic data and transfers zero-shot to real-world images of power lines without any fine-tuning. In this way, we overcome the problem of the limited amount of annotated data for supervised learning.

We believe that our method will contribute to accelerating the deployment of autonomous drones for power line inspection. Our main contributions are:

- A novel system that tightly couples perception and action for autonomous, vision-based power line inspection.
- A model predictive controller that optimizes online the weight of the line tracking and collision avoidance objectives.
- A learning-based power line detector that is trained only on synthetic data and transfers zero-shot to real-world images of power lines.

II. Related Work

An overview of prior works in aerial power line inspection using drones is in [6]. Several planning and control strategies are presented in [9], [10]. A PID controller to control the position and orientation of a quadrotor in relation to the power lines is proposed in [9]. The solution proposed in [10] uses perspective relation and estimation of the position of the next tower to guide the drone. Both works loosely couple perception, planning, and control and consequently either need to have access to an accurate reference trajectory or could result in poor line tracking after the collision avoidance maneuver. A number of works [11], [12], [13], [14], [15] focus on the perception task of detecting and tracking the power lines. Model-based approaches, such as variants of Hough transform and filters, using cameras are proposed in [11], [12], [13]. In spite of their high weight and

* These authors contributed equally. The authors are with the Robotics and Perception Group, Department of Informatics, University of Zurich, and Department of Neuroinformatics, University of Zurich and ETH Zurich, Switzerland (`http://rpg.ifi.uzh.ch`).

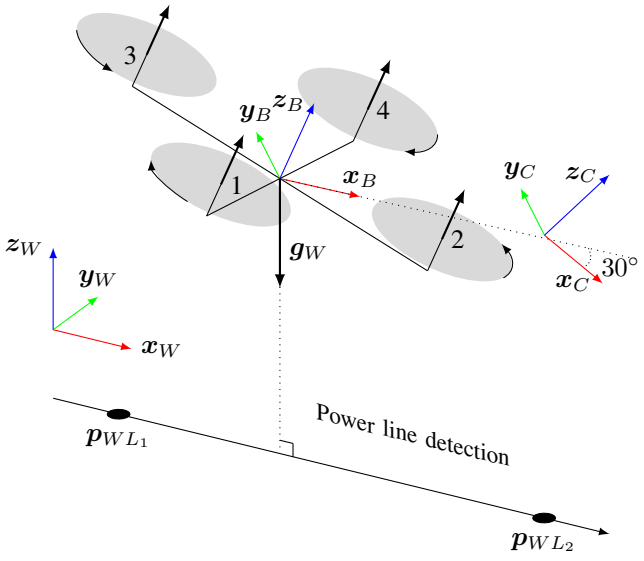

Fig. 1: Diagram of quadrotor and power line model.

computational load, Lidars could also be employed in some specific situations as proposed in [14].

Model predictive control [16] is a powerful solution to couple planning and control for quadrotor autonomous flights. MPC has been used for perching on power lines [17] and agile flights [18]. The first work introducing perception awareness in MPC is [7] where the authors propose to include a perception objective in the MPC to keep a point of interest in the camera field of view. However, we deal with two different perception objectives, line tracking, and collision avoidance, which conflict with each other when the drone approaches the power masts. To enable collision avoidance capabilities, in [19], the authors utilized a chance-constrained MPC formulation. This probabilistic collision constraint allows to account for the perceptual uncertainty and consequently enhances the obstacle avoidance robustness. In [20], an MPC-based reactive planner for visual target tracking and obstacle avoidance is presented. Different from our method, this MPC does not directly generate control commands but planned trajectories, which are tracked by another low-level controller.

III. Methodology

A. Notation

In this manuscript, we define three reference frames. W is the fixed world frame, whose z axis is aligned with the gravity, B is the quadrotor body frame, and C is the camera frame. These reference frames are depicted in Fig. 1. The time derivative of a vector $\boldsymbol{v}$ is represented by $\dot{\boldsymbol{v}}$. In the case of quaternion, the time derivative is defined as $\dot{\boldsymbol{q}} = \frac{1}{2}\Lambda(\boldsymbol{\omega})$, where $\Lambda(\boldsymbol{\omega})$ is the screw-symmetric matrix of the vector $\boldsymbol{\omega}$. The symbol $\odot$ represents the quaternion-vector product. The symbol $\times$ represents the cross product between two vectors.

B. Quadrotor Dynamics

Let $\boldsymbol{p}_{WB}$, $\boldsymbol{q}_{WB}$ and $\boldsymbol{v}_{WB}$ be the position, orientation, and linear velocity of the quadrotor expressed in the world frame W. Let $\boldsymbol{\omega}_B$ be the angular velocity of the body expressed in the body frame B. Additionally, let $c = \Sigma_i c_i$ be the body collective thrust, where c_i is the thrust produced by the i-th motor, $\boldsymbol{c} = \begin{bmatrix}0, 0, c\end{bmatrix}^\intercal$ be the collective thrust vector, m be the mass of the quadrotor, and $\boldsymbol{g}_W$ be the gravity vector. Finally, let $\boldsymbol{J}$ be the diagonal moment of inertia matrix and $\boldsymbol{\tau}_B$ the body collective torque. The quadrotor dynamical model is:

$$\dot{\boldsymbol{x}} = \begin{bmatrix}\dot{\boldsymbol{p}}_{WB} \\ \dot{\boldsymbol{q}}_{WB} \\ \dot{\boldsymbol{v}}_{WB} \\ \dot{\boldsymbol{\omega}}_B\end{bmatrix} = \begin{bmatrix}\boldsymbol{v}_{WB} \\ \frac{1}{2}\Lambda(\omega_B)\cdot\boldsymbol{q}_{WB} \\ \boldsymbol{q}_{WB}\odot\boldsymbol{c}/m + \boldsymbol{g}_W \\ \boldsymbol{J}^{-1}(\boldsymbol{\tau}_B - \boldsymbol{\omega}_B \times \boldsymbol{J}\cdot\boldsymbol{\omega}_B)\end{bmatrix} \tag{1}$$

C. MPC Formulation

The system dynamics in Eq. 1 can be written in compact form as $\dot{\boldsymbol{x}} = f(\boldsymbol{x}, \boldsymbol{u})$. We compute the discrete-time version of it by using a Runge-Kutta method of 4th order with time step dt: $\boldsymbol{x}_{i+1} = f(\boldsymbol{x}_i, \boldsymbol{u}_i, dt)$. The MPC formulation is a non-linear program with quadratic costs:

$$\begin{aligned}\mathcal{L}_{org} = &\bar{\boldsymbol{x}}_N^\intercal \mathcal{Q}_{x,N}\bar{\boldsymbol{x}}_N \ + \sum_{i=0}^{N-1}\left(\bar{\boldsymbol{x}}_i^\intercal\mathcal{Q}_x\bar{\boldsymbol{x}}_i + \bar{\boldsymbol{u}}_i^\intercal\mathcal{R}\bar{\boldsymbol{u}}_i\right)\\ &\arg\min_{\boldsymbol{u}} \ \mathcal{L}_{org}\\ \text{s.t. } &\bar{\boldsymbol{x}}_0 = \boldsymbol{x}_{init}\\ &\boldsymbol{x}_{i+1} = f(\boldsymbol{x}_i, \boldsymbol{u}_i)\\ &\boldsymbol{u}_{\min} \le \boldsymbol{u}_i \le \boldsymbol{u}_{\max}.\end{aligned} \tag{2}$$

D. Perception Objectives

Line Tracking: The purpose of this objective is to keep the power line in the center of the image, to maximize data quality for visual inspection, and to keep a safe distance from the power lines. To this end, we denote the position of the line endpoints in the world frame W as $\boldsymbol{p}_{WL_j}$ $j \in \{1, 2\}$. These points are transformed to the camera frame C to $\boldsymbol{p}_{CL_1}$ and then $\boldsymbol{p}_{CL_2}$ are projected into the image plane coordinates: $[u_1, v_1], [u_2, v_2]$ according to the classical pinhole camera model [21]. The cartesian coordinates are transformed into the polar coordinates as:

$$\theta = \arctan\left(-\frac{u_2 - u_1}{v_2 - v_1}\right),\ r = \left(v_1 - \frac{v_2 - v_1}{u_2 - u_1}u_1\right)\sin\theta. \tag{3}$$

We introduce a new variable $\bar{\boldsymbol{z}}$ in our MPC formulation:

$$\boldsymbol{z} = \begin{pmatrix}\theta \\ r \\ d\end{pmatrix}, \qquad \boldsymbol{z}_s = \begin{pmatrix}0 \\ 0 \\ d_s\end{pmatrix}, \qquad \bar{\boldsymbol{z}} = \boldsymbol{z} - \boldsymbol{z}_s. \tag{4}$$

The variable d represents the distance of the line to the body frame (c.f. Fig. 1) and d_s represents the target value of d. The value of d_s is set by the user according to the desired distance of the flight from the power lines. **Obstacle Avoidance:** Inspired by [22], [23], we include collision avoidance capabilities in our MPC by means of a collision cost and a collision constraint. The collision cost l_o is formulated with the logistic function:

$$l_o = \mathcal{Q}_o/(1 + \exp(\lambda_o\,(d_o - r_o))), \tag{5}$$

where d_o represents the norm of the distance of the body frame to the detected obstacle. The values Q_o, λ_o, r_o are constant quantities that represent weight, smoothness, and distance threshold, respectively. The collision constraint is formulated as a probabilistic chance constraint to account for the uncertainty in the drone state and in the obstacle detection. The objective of this constraint is to ensure that the probability of the collision with an obstacle is less than a predefined threshold: $\Pr\{C_o\} < \delta$. We model obstacles as ellipsoids. Let a_o, b_o, c_o be the semi-principal axes of the ellipsoid modeling an obstacle, and r the radius of a safety area around the quadrotor body frame. The quadrotor is considered to be in collision with the obstacle when:

$$C_o : (\mathbf{p}_{WB} - \mathbf{p}_{WO})^\intercal \, \mathbf{\Omega}_o \, (\mathbf{p}_{WB} - \mathbf{p}_{WO}) \leq 1, \qquad (6)$$

where $\mathbf{\Omega}_o$ is the uncertainty matrix defined as $\mathbf{\Omega}_o = \mathbf{R}_{WO}^\intercal \cdot \text{diag}\left(\frac{1}{(a_o+r)^2}, \frac{1}{(b_o+r)^2}, \frac{1}{(c_o+r)^2}\right) \cdot \mathbf{R}_{WO}$. The quantity $\mathbf{p}_{WO}$ and $\mathbf{R}_{WO}$ represent the position and orientation of the obstacle with respect to the world frame W. Assuming that the quadrotor and obstacle positions are random variables distributed according to Gaussian distributions: $\mathbf{p}_{WB} \sim \mathcal{N}(\hat{\mathbf{p}}_{WB}, \mathbf{\Sigma})$, and $\mathbf{p}_{WO} \sim \mathcal{N}(\hat{\mathbf{p}}_{WO}, \mathbf{\Sigma}_o)$, respectively, we derive the deterministic form of the chance constraint as:

$$\boldsymbol{n}_o^\intercal \mathbf{\Omega}_o^{\frac{1}{2}} (\hat{\boldsymbol{p}}_{WB} - \hat{\boldsymbol{p}}_{WO}) - 1 \geq \text{erf}^{-1}(1-2\delta) \cdot \sqrt{2\boldsymbol{n}_o^\intercal \mathbf{\Omega}_o^{\frac{1}{2}} (\mathbf{\Sigma} + \mathbf{\Sigma}_o) \mathbf{\Omega}_o^{\frac{1}{2}} \boldsymbol{n}_o} \qquad (7)$$

where $\boldsymbol{n}$ is the normalized distance from the body frame to the obstacle and erf(x) is the standard error function for Gaussian distributions [24]. We rearrange Eq. 7 and write it using the shorthand $cc(\hat{\boldsymbol{p}}_{WB}, \Sigma_B, \hat{\boldsymbol{p}}_{WO}, \Sigma_O) \leq 0$ hereafter.

E. Perception-aware MPC for power line inspection

The two perception objectives of line tracking and obstacle avoidance conflict when the quadrotor approaches the power masts. For this reason, finding constant weights to attribute to these objectives in the MPC is difficult. Our solution is to adapt online these weights. To this end, we introduce a new state variable, α. This variable varies in the interval $[0, \alpha_{max}]$. For values close to 0, high priority is given to line tracking. On the contrary, for values close to α_{max}, high priority is given to collision avoidance. The perception-aware MPC proposed in this work is:

$$\begin{aligned}
&\arg\min_{\boldsymbol{u},\alpha} \; \mathcal{L}_{org} + \mathcal{L}_{per} \\
&\mathcal{L}_{per} = \sum_{i=0}^{N-1} \left(\bar{\alpha}_i^2 \bar{\boldsymbol{z}}_i^\intercal \mathcal{Q}_p \bar{\boldsymbol{z}}_i + l_o + \mathcal{Q}_\alpha \alpha_i^2\right) \\
&\quad \text{s.t. } \bar{\boldsymbol{x}}_0 = \boldsymbol{x}_{init} \\
&\qquad \boldsymbol{x}_{i+1} = f(\boldsymbol{x}_i, \boldsymbol{u}_i) \\
&\qquad \boldsymbol{u}_{\min} \leq \boldsymbol{u}_i \leq \boldsymbol{u}_{\max} \\
&\quad cc(\hat{\boldsymbol{p}}_{WB,i}, \Sigma_{B,i}, \hat{\boldsymbol{p}}_{WO,i}, \Sigma_{O,i}) + c\bar{\alpha}_i \leq 0 \\
&\qquad 0 \leq \alpha_i \leq \alpha_{max},
\end{aligned} \qquad (8)$$

where $\bar{\alpha} = 1 - \alpha/\alpha_{max}$ and c is a constant value that is used to weight the priority of the chance constraint.

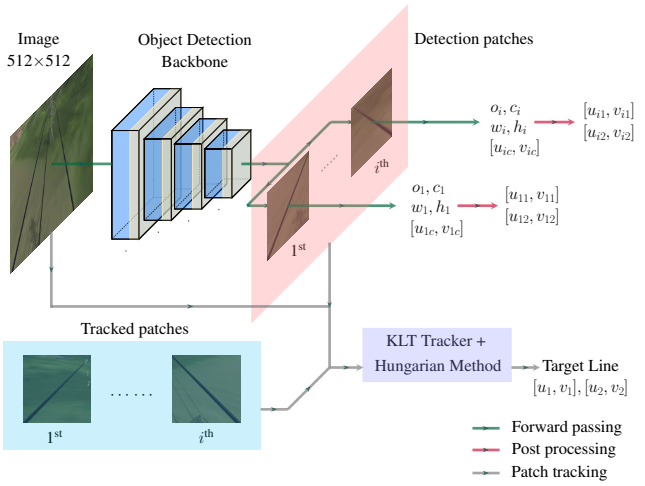

Fig. 2: Overview of our learning-based power line detector and tracker. The detector takes a single RGB image as input and outputs end points of the detected power lines in pixel coordinates. The center patch of each detection is matched with the prediction of the previous patch using the Hungarian method [26]. We use a KLT tracker [27] to perform tracking. The final output is the tracked lines endpoints which are given to the MPC.

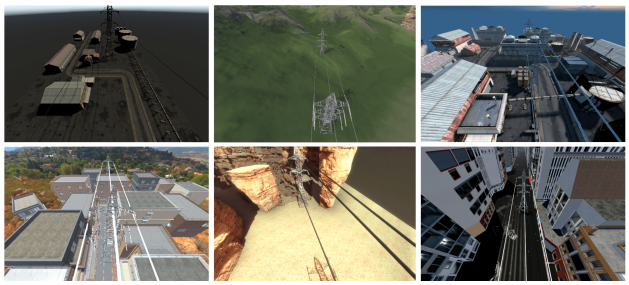

Fig. 3: Sample images from the proposed power line dataset.

F. Line Detection and Tracking

In this work, we propose a novel deep-learning-based power line detector based on the object detector [8], [25]. As shown in Fig. 2, our detector takes monocular RGB images as input and outputs: (i) width w_i and height w_i of the bounding boxes that fully contain the detected power line, where i indicates the number of detection; (ii) the inclination of the line o_i (either +1 or -1). The endpoints of positive inclined lines, i.e., $o_i = +1$, correspond to the top-left and bottom-right corners of the bounding box. The endpoints of negative inclined lines correspond to the top-right and bottom-left corners of the bounding box; (iii) the center of the line $[u_{ic}, v_{ic}]$; (iv) the confidence score c of the prediction. If the confidence score is not larger than a predefined threshold (we use 0.8 in all our experiments), the detection is labeled as invalid and is not used. To perform tracking, we use a tracking-by-detection approach to track the detected power lines. We collected a dataset of ∼30k images of labeled power lines of different colors and thicknesses in different 6 environments (c.f. Fig. 3).

IV. Experiments

Benefits of our learning-based line detector: In these experiments, we compare the proposed learning-based line detector against a traditional line detector approach based on

Method	Chamfer Distance			EA Score		
	P	R	F	P	R	F
Hough	0.70	0.32	0.44	0.46	0.19	0.28
P-Hough	0.26	0.31	0.28	0.10	0.16	0.10
Ours	**0.92**	**0.77**	**0.84**	**0.93**	**0.78**	**0.85**
Improvement (%)	31	141	91	102	311	204

TABLE I: Quantitative evaluation of the performance of the proposed learning-based line detector and of the classical approaches.

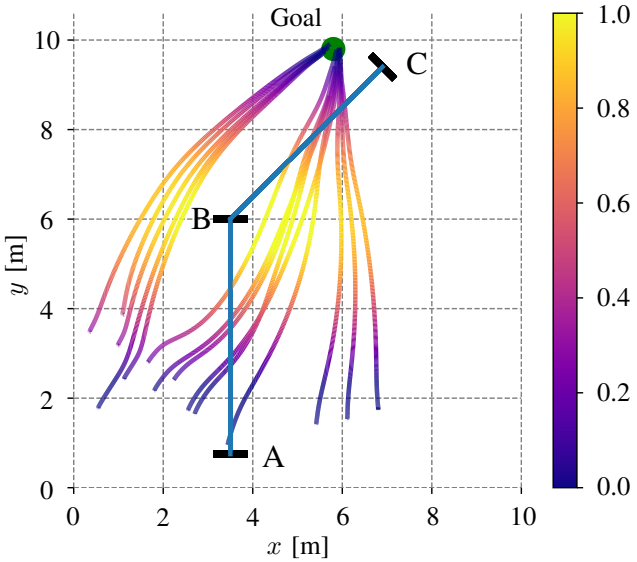

Fig. 4: Visualization of the flown trajectories color-coded according to the values of α, c.f. Sec. III-E. Our MPC is able to find collision-free trajectories starting from non-collision-free reference trajectories.

the Hough transform algorithm [28]. We design a traditional line detection baseline that uses the Canny edge detector algorithm [29] to detect edge features in the image and the Hough transform algorithm to estimate the line parameters. We also design a probabilistic version of this algorithm, Probabilistic Hough Transform (P-Hough), that runs on a sampled subset of the detected edges. The dimension of this subset depends on predefined thresholds that vary according to the number of detected edges. The parameters of the traditional approach were tuned on the training sequences of our simulated power line dataset. The results on the test sequences are listed in Table I. We use the metrics proposed in [30], which are the Precision, Recall, and the F1 score of the line matching results based on Chamfer distance and EA score [30]. Our line detector greatly outperforms the traditional approach.

Robustness to unknown location of the power masts:

In this experimental setting, we evaluate the performance of our system in the case where the initial reference trajectory is in collision with the power masts. We run our tests within the Flightmare simulation environment and assume that the MPC has access to the ground truth obstacle position and only vary the reference trajectory. We designed an environment with 3 power masts (labelled A, B, C) as shown in Fig. 4. We randomly sampled 100 starting points in a rectangular region of size 8×3 m in the vicinity of the power mast A (the center of A is located in the middle of the bottom edge of this rectangular region). The endpoint is fixed 1 m away from the left side of the power mast C. The reference trajectory given to the MPC is a straight line connecting the starting and end points with no yaw change. Some of these reference trajectories are in collision with the power mast B. Our system achieves a 100% success rate, i.e. no collision with the power masts. We show in Fig. 4, 13 flown trajectories.

	Simple	Warehouse	Forest	Village	Mean
Our MPC	**0.74**	**0.63**	**0.61**	**0.67**	**0.67**
Classical MPC	0.53	0.49	0.44	0.45	0.48

TABLE II: Quantitative comparison of the proposed perception-aware MPC (Eq. 8) against the classical MPC formulation (Eq. 2). The evaluation metric refers to the visibility of the line (Eq. 9).

Benefits of tightly-coupling perception and action: In this experiment, we evaluate the benefits of tightly-coupling perception, planning, and control in terms of the visibility of the power lines compared to the classical MPC formulation. We use the proposed learning-based line detector and assume that the MPC has access to the ground-truth position of the power masts. We use the similarity score $\mathcal{S}$ as the evaluation metric, which is defined as:

$$\mathcal{S}_\theta = 1 - \frac{2\theta}{\pi},\ \mathcal{S}_d = 1 - \frac{h}{\sqrt{w^2 + l^2}},\ \mathcal{S} = (\mathcal{S}_\theta \cdot \mathcal{S}_d)^2 \quad (9)$$

where θ is the normalized angular distance between the detected and the reference line, and h is the normalized distance between the center points of the lines. The quantity h is normalized by the length of the image diagonal, where w and l are the image width and height, respectively. The results are in Table II. Our perception-aware MPC improves the line visibility on average by 40%.

V. Conclusions

In this work, we present a system for autonomous power line inspection using perception-aware MPC. Our approach generates control commands that maximize the visibility of the power lines while safely avoiding the power masts. Our MPC formulation includes two perception objectives, one for line tracking and one for obstacle avoidance. The MPC adapts the weights of these two objectives online. To detect the power lines, we propose a novel learning-based detector. This learning-based detector is only trained on synthetic data and is able to transfer to real-world images without any fine-tuning. We show that our system is robust to unknown information on the position of the power lines and power masts. We also show that our perception-aware MPC improves power line visibility by 40%. We demonstrate a real-world application in a mock-up power line environment. Future improvements for our system might include i) improving system robustness against disturbances such as wind [31], model mismatch [32] or sensor failures [33] and ii) perching on the power line [17] in order to recharge the battery on the fly [34].

REFERENCES

[1] "Drone industry insights - drones in the energy industry: The energy drone operator benchmark," http://droneii.com.

[2] E. Commission, "Drone strategy 2.0: Creating a large-scale european drone market," https://ec.europa.eu/commission/presscorner/detail/en/ip_22_7076, accessed: 2023-02-13.

[3] "U.s. electric system is made up of interconnections and balancing authorities," https://www.eia.gov/todayinenergy/detail.php?id=27152.

[4] "Power distribution in europe facts and figures," https://cdn.eurelectric.org/media/1835/dso_report-web_final-2013-030-0764-01-e-h-D66B0486.pdf.

[5] "California's second-largest wildfire was sparked when power lines came in contact with a tree, cal fire says," https://edition.cnn.com/2022/01/05/us/dixie-fire-power-lines-cause-pge.

[6] V. N. Nguyen, R. Jenssen, and D. Roverso, "Automatic autonomous vision-based power line inspection: A review of current status and the potential role of deep learning," *International Journal of Electrical Power & Energy Systems*, vol. 99, pp. 107–120, 2018.

[7] D. Falanga, P. Foehn, P. Lu, and D. Scaramuzza, "Pampc: Perception-aware model predictive control for quadrotors," in *IEEE/RSJ Int. Conf. Intell. Robot. Syst. (IROS)*, 2018, pp. 1–8.

[8] J. Redmon, S. Divvala, R. Girshick, and A. Farhadi, "You only look once: Unified, real-time object detection," in *Proceedings of the IEEE conference on computer vision and pattern recognition*, 2016.

[9] K. Takaya, H. Ohta, V. Kroumov, K. Shibayama, and M. Nakamura, "Development of uav system for autonomous power line inspection," in *2019 23rd International Conference on System Theory, Control and Computing (ICSTCC)*. IEEE, 2019, pp. 762–767.

[10] X. Hui, J. Bian, Y. Yu, X. Zhao, and M. Tan, "A novel autonomous navigation approach for uav power line inspection," in *2017 IEEE International Conference on Robotics and Biomimetics (ROBIO)*. IEEE, 2017, pp. 634–639.

[11] M. Nasseri, H. Moradi, S. Nasiri, and R. Hosseini, "Power line detection and tracking using hough transform and particle filter," in *2018 6th RSI International Conference on Robotics and Mechatronics (IcRoM)*. IEEE, 2018, pp. 130–134.

[12] F. Tian, Y. Wang, and L. Zhu, "Power line recognition and tracking method for uavs inspection," in *2015 IEEE International Conference on Information and Automation*. IEEE, 2015, pp. 2136–2141.

[13] M. Gerke and P. Seibold, "Visual inspection of power lines by uas," in *2014 International Conference and Exposition on Electrical and Power Engineering (EPE)*. IEEE, 2014, pp. 1077–1082.

[14] F. Azevedo, A. Dias, J. Almeida, A. Oliveira, A. Ferreira, T. Santos, A. Martins, and E. Silva, "Lidar-based real-time detection and modeling of power lines for unmanned aerial vehicles," *Sensors*, 2019.

[15] A. Dietsche, G. Cioffi, J. Hidalgo-Carrió, and D. Scaramuzza, "Powerline tracking with event cameras," in *2021 IEEE/RSJ International Conference on Intelligent Robots and Systems (IROS)*. IEEE, 2021.

[16] H. Nguyen, M. Kamel, K. Alexis, and R. Siegwart, "Model predictive control for micro aerial vehicles: A survey," in *2021 European Control Conference (ECC)*. IEEE, 2021, pp. 1556–1563.

[17] J. L. Paneque, J. R. Martínez-de Dios, A. Ollero, D. Hanover, S. Sun, A. Romero, and D. Scaramuzza, "Perception-aware perching on powerlines with multirotors," *IEEE Robotics and Automation Letters*, vol. 7, no. 2, pp. 3077–3084, 2022.

[18] A. Romero, S. Sun, P. Foehn, and D. Scaramuzza, "Model predictive contouring control for time-optimal quadrotor flight," *IEEE Transactions on Robotics*, 2022.

[19] A. T. Schwarm and M. Nikolaou, "Chance-constrained model predictive control," *AIChE Journal*, vol. 45, no. 8, pp. 1743–1752, 1999.

[20] B. Penin, P. R. Giordano, and F. Chaumette, "Vision-based reactive planning for aggressive target tracking while avoiding collisions and occlusions," *IEEE Robot. Autom. Lett.*, vol. 3, no. 4, 2018.

[21] R. Szeliski, *Computer Vision: Algorithms and Applications*, ser. Texts in Computer Science. Springer, 2010.

[22] H. Zhu and J. Alonso-Mora, "Chance-constrained collision avoidance for mavs in dynamic environments," *IEEE Robotics and Automation Letters*, vol. 4, no. 2, pp. 776–783, 2019.

[23] J. Lin, H. Zhu, and J. Alonso-Mora, "Robust vision-based obstacle avoidance for micro aerial vehicles in dynamic environments," in *2020 IEEE International Conference on Robotics and Automation (ICRA)*. IEEE, 2020, pp. 2682–2688.

[24] T. D. Barfoot, *State Estimation for Robotics - A Matrix Lie Group Approach*. Cambridge University Press, 2015.

[25] G. Jocher, A. Chaurasia, A. Stoken, J. Borovec, NanoCode012, Y. Kwon, TaoXie, K. Michael, J. Fang, imyhxy, Lorna, C. Wong, Z. Yifu, A. V, D. Montes, Z. Wang, C. Fati, J. Nadar, Laughing, UnglvKitDe, tkianai, yxNONG, P. Skalski, A. Hogan, M. Strobel, M. Jain, L. Mammana, and xylieong, "ultralytics/yolov5: v6.2 - yolov5 classification models, apple m1, reproducibility, clearml and deci.ai integrations," 2022. [Online]. Available: https://doi.org/10.5281/zenodo.7002879

[26] H. W. Kuhn, "The hungarian method for the assignment problem," *Naval research logistics quarterly*, vol. 2, no. 1-2, pp. 83–97, 1955.

[27] B. D. Lucas and T. Kanade, "An iterative image registration technique with an application to stereo vision," in *IJCAI'81: 7th international joint conference on Artificial intelligence*, vol. 2, 1981, pp. 674–679.

[28] J. Illingworth and J. Kittler, "A survey of the hough transform," *Computer vision, graphics, and image processing*, vol. 44, no. 1, 1988.

[29] P. Bao, L. Zhang, and X. Wu, "Canny edge detection enhancement by scale multiplication," *IEEE transactions on pattern analysis and machine intelligence*, vol. 27, no. 9, pp. 1485–1490, 2005.

[30] K. Zhao, Q. Han, C.-B. Zhang, J. Xu, and M.-M. Cheng, "Deep hough transform for semantic line detection," *IEEE Transactions on Pattern Analysis and Machine Intelligence*, 2021.

[31] G. Cioffi, L. Bauersfeld, and D. Scaramuzza, "Hdvio: Improving localization and disturbance estimation with hybrid dynamics vio," *Robotics: Science and Systems*, 2023.

[32] L. Bauersfeld, E. Kaufmann, P. Foehn, S. Sun, and D. Scaramuzza, "Neurobem: Hybrid aerodynamic quadrotor model," *Robotics: Science and Systems*, 2021.

[33] B. Sun, J. Xing, H. Blum, R. Siegwart, and C. Cadena, "See yourself in others: Attending multiple tasks for own failure detection," in *2022 International Conference on Robotics and Automation (ICRA)*. IEEE, 2022, pp. 8409–8416.

[34] R. Kitchen, N. Bierwolf, S. Harbertson, B. Platt, D. Owen, K. Griessmann, and M. A. Minor, "Design and evaluation of a perching hexacopter drone for energy harvesting from power lines," in *2020 IEEE/RSJ International Conference on Intelligent Robots and Systems (IROS)*. IEEE, 2020, pp. 1192–1198.